An early Eocene carbon cycle perturbation at ~52.5 Ma in the Southern Alps: Chronology and biotic response

Claudia Agnini,[1,2] Patrizia Macrì,[3] Jan Backman,[4] Henk Brinkhuis,[5] Eliana Fornaciari,[1] Luca Giusberti,[1] Valeria Luciani,[6] Domenico Rio,[1] Appy Sluijs,[5] and Fabio Speranza[3]

Received 11 June 2008; revised 4 February 2009; accepted 4 March 2009; published 14 May 2009.

[1] At least two transient events of extreme global warming occurred superimposed on the long-term latest Paleocene and early Eocene warming trend in the Paleocene-Eocene thermal maximum (PETM) (or ETM1 ~55.5 Ma) and the Elmo (or ETM2 ~53.6 Ma). Other than warmth, the best known PETM is characterized by (1) significant injection of ^{13}C-depleted carbon into the ocean-atmosphere system, (2) deep-sea carbonate dissolution, (3) strong biotic responses, and (4) perturbations of the hydrological cycle. Documentation of the other documented and suspected ''hyperthermals'' is, as yet, insufficient to assess whether they are similar in nature to the PETM. Here we present and discuss biomagnetostratigraphic data and geochemical records across two lower Eocene successions deposited on a continental margin of the western Tethys: the Farra and Possagno sections in the Venetian pre-Alps. We recognize four negative carbon isotope excursions within chron C24. Three of these shifts correlate to known or suspected hyperthermals: the PETM, the Eocene thermal maximum 2 (~53.6 Ma), and the informally named ''X event'' (~52.5 Ma). The fourth excursion lies within a reverse subchron and occurred between the latter two. In the Farra section, the X event is marked by a ~0.6‰ negative carbon isotope excursion and carbonate dissolution. Furthermore, the event exhibits responses among calcareous nannofossils, planktic foraminifera, and dinoflagellates that are similar to, though less intense than, those observed across the PETM. Sedimentological and quantitative micropaleontological data from the Farra section also suggest increased weathering and runoff as well as sea surface eutrophication during this event.

Citation: Agnini, C., P. Macrì, J. Backman, H. Brinkhuis, E. Fornaciari, L. Giusberti, V. Luciani, D. Rio, A. Sluijs, and F. Speranza (2009), An early Eocene carbon cycle perturbation at ~52.5 Ma in the Southern Alps: Chronology and biotic response, *Paleoceanography*, *24*, PA2209, doi:10.1029/2008PA001649.

1. Introduction

[2] Deep-sea oxygen isotope records suggest a ~7 Ma long warming trend from the late Paleocene through the early Eocene (ca. 59–52 Ma) that peaked at the Early Eocene Climatic Optimum (EECO) [*Zachos et al.*, 2001]. Superimposed on this trend were at least two short (<200 ka) episodes of extreme global warming, the PETM at ca. 55.5 Ma and the Eocene thermal maximum 2 (ETM2; also referred to as Elmo, H-1) at ca. 53,6 Ma [*Kennett and Stott*, 1991; *Thomas and Zachos*, 2000; *Bralower et al.*, 2002; *Lourens et al.*, 2005]. These events, called hyperthermals, have become a focal point of research because they are related to abrupt and massive releases of ^{13}C-depleted carbon into the ocean-atmosphere system [*Dickens et al.*, 1995; *Lourens et al.*, 2005; *Nicolo et al.*, 2007], major perturbations of biota and the hydrological cycle [*Bowen et al.*, 2006; *Pagani et al.*, 2006; *Sluijs et al.*, 2007a]. The input of carbon is evidenced by prominent negative carbon isotope excursions (CIEs) in carbonate and organic matter, as well as dissolution of carbonate in deep-sea sediments [*Zachos et al.*, 2005; *Pagani et al.*, 2006; *Schouten et al.*, 2007]. Although the source and mass of carbon involved remain contentious, the amount of injected carbon during the PETM is comparable within a factor of two to that expected from anthropogenic carbon emissions [*Dickens et al.*, 1995, 1997; *Raven et al.*, 2005; *Kleypas et al.*, 2006; *Denman et al.*, 2007; *Jansen et al.*, 2007].

[3] Available information, albeit somewhat tentative, suggest that other brief intervals in the early Paleogene may also be characterized by elevated sea surface temperatures, negative CIEs, deep-sea carbonate dissolution and biotic perturbations [*Thomas and Zachos*, 2000; *Thomas et al.*, 2000; *Cramer et al.*, 2003; *Zachos et al.*, 2004; *Röhl et al.*, 2005; *Coccioni et al.*, 2006; *Thomas et al.*, 2006; *Nicolo et al.*, 2007; *Quillévéré et al.*, 2008]. In coastal to hemipelagic settings, these lesser events may also contain evidence of increased continental weathering [*Nicolo et al.*, 2007]. These suspected hyperthermals include an event ca. 53.2 Ma termed I [*Cramer et al.*, 2003; *Nicolo et al.*, 2007] and an event ca. 52.5 Ma called K or X [*Röhl et al.*, 2005; *Thomas et al.*, 2006]. Presently, however, the precise

[1]Dipartimento di Geoscienze, Università di Padova, Padua, Italy.
[2]Istituto di Geoscienze e Georisorse, CNR-Padova, Dipartimento di Geoscienze, Università di Padova, Padua, Italy.
[3]Istituto Nazionale di Geofisica e Vulcanologia, Rome, Italy.
[4]Department of Geology and Geochemistry, Stockholm University, Stockholm, Sweden.
[5]Palaeoecology, Laboratory of Palaeobotany and Palynology, Institute of Environmental Biology, Utrecht University, Utrecht, Netherlands.
[6]Dipartimento di Scienze della Terra, Polo Scientifico Tecnologico, Università di Ferrara, Ferrara, Italy.

0883-8305/09/2008PA001649$12.00

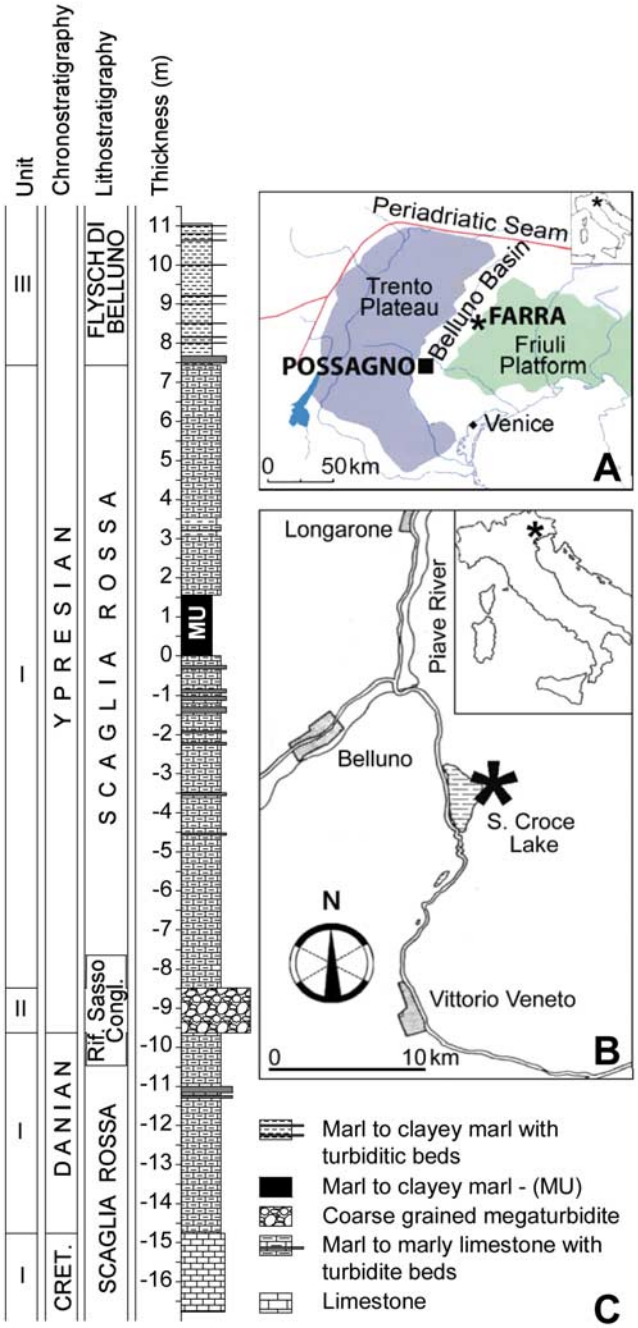

Figure 1. (a) Paleogeographic context of the Farra and Possagno sections. The main late Cretaceous–early Paleogene paleogeographic elements of the Southern Alps are shown (adapted from *Cati et al.* [1989]). The locations of the two studied sections are also reported. (b) Geographic location of the Farra d'Alpago section. (c) Lithological log of the Farra section is plotted against lithostratigraphy and chronostratigraphy.

number of such events, their ages and durations, and their characteristics remain uncertain. Moreover, it is not obvious whether they are all truly global in nature and causally related [*Cramer et al.*, 2003; *Nicolo et al.*, 2007; *Westerhold et al.*, 2007; *Quillévéré et al.*, 2008]. In part, this is because the lesser events have been documented mostly from condensed deep-sea settings, where incomplete recovery and dissolution have impacted sedimentary records [*Nicolo et al.*, 2007]. Much work remains to be done from a wide variety of stratigraphic sections to understand the nature of early Paleogene hyperthermals.

[4] To address this issue, we are currently studying several complete and relatively expanded lower Eocene stratigraphic outcrops in the Venetian Alps of northeast Italy. Two of these sections are near Possagno and Farra d'Alpago, hereafter referred to as Farra (Figure 1). New stable isotope data from the Possagno section is presented to better constrain the number and relative position of carbon isotope excursions within chron C24 (55.5 – 52.5 Ma). At Farra, we have generated an integrated paleomagnetic, biostratigraphic and stable isotope stratigraphic framework. Geochemical proxies, including stable isotopes and $CaCO_3$ content of bulk sediment, have been used to examine aberrations in the global exogenic carbon pool and climate. Calcareous nannofossil, planktic foraminifera and organic dinoflagellate cyst (dinocyst) data have also been generated to assess biotic changes in the surface waters. We identify four events and the X event is exceptionally well recorded in the Farra section, where is it characterized by a negative carbon isotope excursion, deep-sea carbonate dissolution at its onset, transient changes in planktic marine biota and a significant increase in terrigenous discharge to the sea.

2. Materials and Methods

2.1. Materials

[5] The Possagno section is located at 45°51′26″N 11°52′58″E in the Carcoselle quarry, 1.5 km west of the town of Possagno (Treviso, NE Italy; Figure 1). The Possagno section belongs to a Mesozoic–Cenozoic pelagic-hemipelagic sequence in the Belluno Basin, delimited to the west by the Trento Plateau and to the east by the Friuli Platform (Figure 1a) [*Arenillas et al.*, 1999; *Agnini et al.*, 2006b]. Although the Possagno section is characterized by low sedimentation rate of ca. 0.5 cm/ka, it provides a continuous record extending from chron C24r to chron C23r. Detailed description of this section and interpretation of its depositional setting have been reported previously [*Bolli*, 1975; *Arenillas et al.*, 1999; *Agnini et al.*, 2006b]. The overall section can be described as pink-reddish limestone to calcareous marlstone and this pelagic to hemipelagic succession is ascribed to the Scaglia Rossa. Several marly horizons occur between 8 m level to ca. 14m level within chron C24. New stable isotope data are thus generated for this section with the aim of better constraining and characterizing the early Eocene hyperthermals.

[6] The Farra section is located at 46°06′58″N 12°22′42″E, 1.5 km east of the Farra d'Alpago village along the Runal Rivulet (Figures 1a and 1b). The section is divided into three lithologic units. Unit I consists of pink-reddish limestone to red finely bedded marl (the Scaglia Rossa). The basal 7 m of the section (Unit I) has approximately 2 m of Maastrichtian pink-reddish limestone overlain by approximately 5m of Danian marly limestone. The Danian sediments are followed by Unit II, an approximately

1 m thick coarse-grained turbidite referred to as Conglomerato di Rifugio Sasso [*Mantovani et al.*, 1978]. The reappearance of hemipelagic deposition, just above Unit II, consists of ca. 14 m of finely bedded lower Eocene red calcareous marls. Given similarities to underlying lithology, it has also been ascribed to Unit I. A ca. 1.5 m thick subunit, where a decrease in the $CaCO_3$ content is evident, occurs within Unit I, starting at relative depth 0 m, here termed the marly unit (MU) (Figure 1). This prominent change in lithology is characterized by four alternating red and green clayey marl layers. In the upper part of the Farra section, the Scaglia Rossa of Unit I is overlain by the Flysch di Belluno (Unit III), which is mainly composed of marl to clayey marl with common turbiditic beds (Figure 1c) [*Agnini et al.*, 2006a]. Foraminifera-based estimates of paleobathymetry suggest that the Farra section was deposited in upper middle bathyal depths (see discussion for details).

2.2. Methods

2.2.1. Geochemical Analyses

[7] Bulk rock samples were analyzed for oxygen and carbon stable isotopes from the Possagno section (N = 53) and the Farra section (N = 70), using a mass spectrometer (Finnigan MAT 252) equipped with a Kiel device at the Department of Geology and Geochemistry of Stockholm University. Carbon and oxygen isotopes values were calibrated to the Vienna Pee Dee Belemnite standard (VPDB) and converted to conventional delta notation ($\delta^{13}C$ and $\delta^{18}O$). Analytical precision is within ±0.06‰ for $\delta^{13}C$ and ±0.07‰ for $\delta^{18}O$, respectively. Coulometry was used to determine calcium carbonate content (wt %) in the Farra section. Analytical precision is within ±0.8%. Geochemical data are reported in Data Set S1.[1]

2.2.2. Calcareous Nannofossil at Farra

[8] Standard smear slides were prepared from 86 samples. Assemblage studies were based on counts of, at least, a total of 300 specimens [*Thierstein et al.*, 1977] from 66 samples by means of light microscopy at a magnification of 1250x. The abundance patterns of *Sphenolithus radians* and *Girgisia gammation* were determined by counting index species in a prefixed area (1 mm^{-2}) [*Backman and Shackleton*, 1983], whereas the abundances of rare taxa such as *Chiphragmalithus, Discoaster diastypus*, *Discoaster lodoensis* and *Tribrachiatus orthostylus* were determined by counting the index species along three smear slide transects, on each of the 86 smear slides. The taxonomy used is described by *Aubry* [1984, 1988, 1989, 1990, 1999] and *Perch-Nielsen* [1985], and the zonal scheme used is that of *Martini* [1971]. Analytical calcareous nannofossil data are reported in Data Set S2.

2.2.3. Planktic and Benthic Foraminifera and Biosilica at Farra

[9] Planktic foraminiferal analyses were carried out on 33 samples from a ~11 m thick interval straddling the marly unit, whereas benthic foraminifera were examined in 18 samples from a ~4 m thick interval straddling the base of the marly unit. Foraminifera were extracted from most of the indurated marls and limestones using the "cold acetolyze" technique of *Lirer* [2000]. The soft marly samples were treated using standard methods: disaggregation with hydrogen peroxide at concentrations varying from 10 to 30% (Data Set S3).

[10] Planktic and benthic foraminifera have been analyzed in the >63 μm fraction by counting, where possible, the relative abundance of genera and species (%) in a population of about 300 specimens each for planktics and benthics (Data Sets S3 and S4). The fragmentation index (F index) is calculated by counting the number of planktic foraminiferal fragments or partially dissolved tests versus entire tests, using a total of about 300 planktic foraminifera and fragments/dissolved tests [*Hancock and Dickens*, 2005]. Abundances of biosiliceous components, radiolaria and sponge spicules, are reported as percentages with respect to the total planktic assemblage: foraminifera plus biosiliceous fraction. The planktic foraminiferal zonal scheme is that of *Berggren and Pearson* [2005]. We allocate all specimens of benthic foraminifera to morphogroups, mainly following *Alegret et al.* [2003] and *Kaminski and Gradstein* [2005], in order to estimate the infaunal/epifaunal ratio.

2.2.4. Dinocysts at Farra

[11] Dinocysts were examined in 27 samples using established palynological processing methods [*Sluijs et al.*, 2003]. Briefly, samples were freeze-dried and a known amount of *Lycopodium* spores were added to ca. 10 g of material. Then the samples were treated with 30% HCl and twice with 38% HF for carbonate and silicate removal, respectively. Residues were sieved using a 15 μm nylon mesh to remove small particles. To break up clumps of residue, the sample was placed in an ultrasonic bath for a maximum of 5 min, sieved again, and subsequently concentrated to 1 ml, of which 10–35 μl was mounted on microscope slides. Taxonomy follows that cited by *Fensome and Williams* [2004]. Analytical data are reported in Data Set S5.

2.2.5. Magnetostratigraphy at Farra

[12] We analyzed 52 samples (21 drilled and 31 hand sampled), adopting a sampling interval of ca. 30 cm. The samples were oriented in situ before extraction by a magnetic compass, corrected to account for the mean magnetic declination of the geomagnetic field in the site section during the year 2006 [*Istituto Nazionale di Geofisica e Vulcanologia*, 2007]. Paleomagnetic measurements were carried out in a shielded room of the paleomagnetic laboratory at the Istituto Nazionale di Geofisica e Vulcanologia in Rome, using an automated pass through 2-G Enterprises DC SQUID cryogenic magnetometer. The characteristic remanent magnetization directions (ChRMs) from the studied sediments were isolated by means of a thermal demagnetization in 11 steps, from 20° to 650°C. Demagnetization data were plotted on both orthogonal demagnetization diagrams [*Zijderveld*, 1967] and on equal-area projections (Figures 2a–2d), and the magnetization components were isolated by principal component analysis [*Kirschvink*, 1980].

3. Results

3.1. Geochemistry at Possagno and Farra

[13] At Possagno, the $\delta^{13}C$ data show a negative shift of about 1.5‰ at the 0 m level, which corresponds to the

[1] Auxiliary materials are available at ftp://ftp.agu.org/apend/pa/2008pa001649.

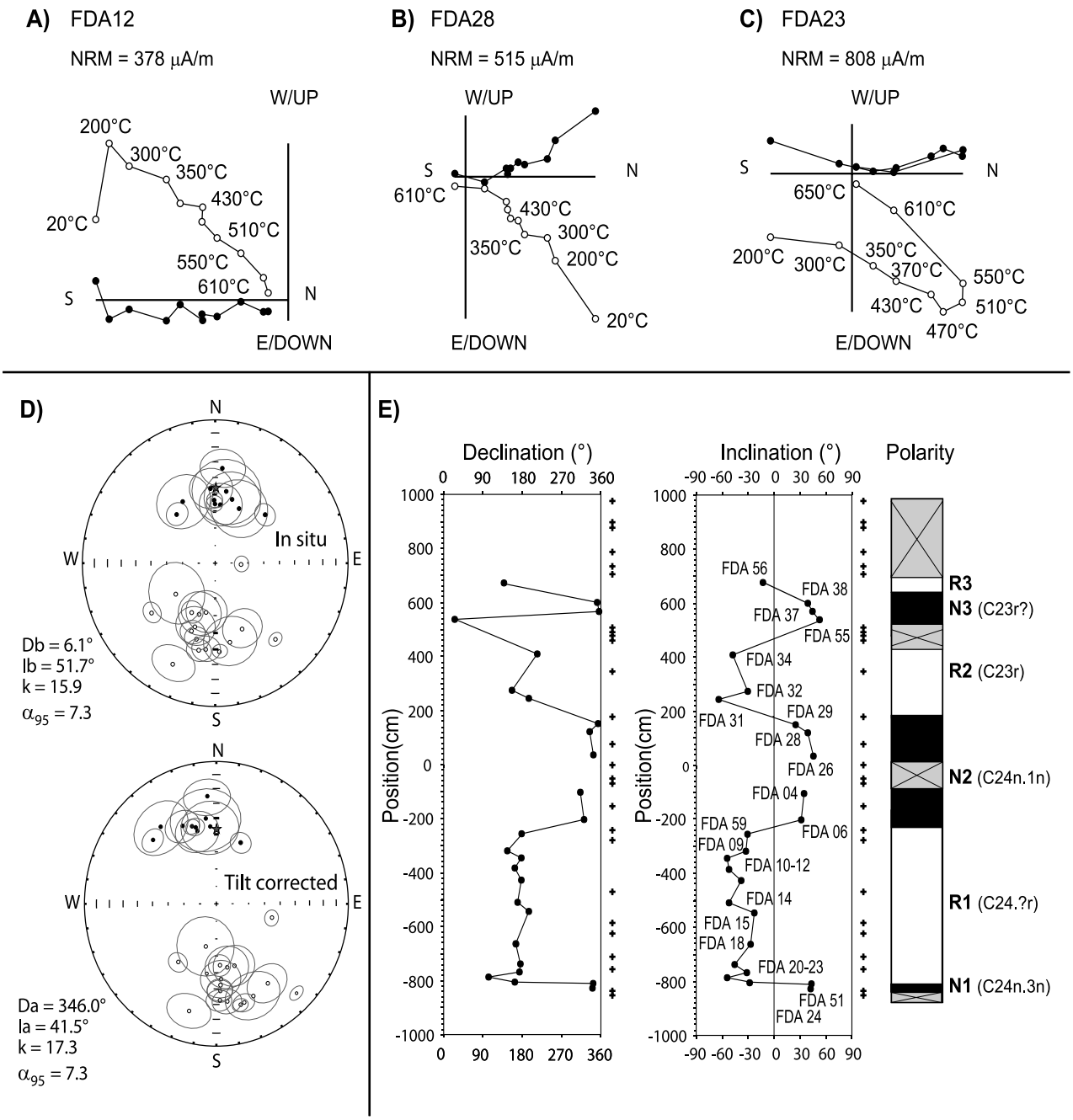

Figure 2. Paleomagnetic results from the Farra d'Alpago section. (a–c) Orthogonal vector diagrams of typical thermal demagnetization data, tilt-corrected coordinates. Open (solid) circles represent projections on the vertical (horizontal) plane. The samples in Figures 2a and 2b are characterized by a reverse and normal polarity ChRM, respectively; the sample in Figure 2c yields a reverse and a normal polarity component in the 300°–470°C and 550°–650°C temperature intervals, respectively. The components defined at lower and higher unblocking temperatures are likely carried by titanomagnetite and hematite, respectively. The high-temperature normal polarity component is due to magnetic overprint. (d) Equal-area projections of the ChRMs from the individual paleomagnetic samples. Open (solid) circles represent projection onto the upper (lower) hemisphere, ellipses represent the maximum angular dispersion (MAD) values about each ChRM direction, and the star represents the normal polarity geocentric axial dipole (GAD) magnetic field direction for the study area. ChRMs are shown before (Db and Ib) and after (Da and Ia) tilt correction; value k and α_{95} are statistical parameters after *Fisher* [1953]. (e) Tilt-corrected ChRMs and magnetic polarity zones plotted along the stratigraphic positions (black, normal; white, reverse; gray and crosshatched, indeterminate). The crosses indicate failed samples. Correlative polarity chrons (following *Cande and Kent* [1995]) are in parentheses after the polarity zone labels.

Paleocene-Eocene boundary [*Agnini et al.*, 2006b] (Figure 3). There are additional, minor negative carbon excursions above the Paleocene-Eocene boundary. The first one, ~0.4‰ at the ~8 m level, falls within the uppermost part of chron C24r, the second one, ~0.3–0.4‰ at the ~10.5 m level, occurs within subchron C24n.3n, the third one, ~0.4‰ at ~ the 12.5 m level, lies within subchron C24n.2n, and the fourth one, ~0.4‰ at ~ the 14.8 m level, is recorded in subchron C24n.1n, according to biomagnetostratigraphic data [*Agnini et al.*, 2006b].

[14] At Farra, we record a long-term $\delta^{13}C$ decreasing trend across the lower Eocene, which is interrupted by a transient but significant negative carbon shift of ~0.6‰ at the −1 cm level, which effectively coinciding with the lower boundary of the marly unit (Figure 3). This amplitude of isotopic change is similar to that recorded for the X event in the South Atlantic and the K event in the Pacific [*Cramer et al.*, 2003; *Röhl et al.*, 2004, 2005; *Thomas et al.*, 2006]. The ~0.6 ‰ negative $\delta^{13}C$ excursion is followed by a gradual recovery to preevent conditions. An abrupt decrease in $CaCO_3$ content from approximately 70% to 25% corresponds to the $\delta^{13}C$ excursion, marking the onset of the marly unit (Figure 4). The $CaCO_3$ values remain low across the $\delta^{13}C$ excursion, that is from the 0cm level to the +150cm level. The $\delta^{18}O$ values show wide scatter throughout the section, ranging between −0.8 and −3.0‰, with relatively high values within the marly unit (Figure 3). This pattern may indicate that diagenesis has affected the original isotopic signal [*Schmitz et al.*, 1997]. The interval between the onset of the $\delta^{13}C$ negative excursion and its recovery, that is from the -1 cm level to the +150 cm level, is the main focus of this paper.

3.2. Calcareous Nannofossils at Farra

[15] Calcareous nannofossil assemblages are rich and well diversified. Preservation varies from poor to moderate except for the lowermost part of the marly unit, where dissolution is more intense. The assemblages also show a transient and striking modification that is constrained to the marly unit. Specifically, *Coccolithus pelagicus*, reworked species and, subordinately, *Ericsonia,* increase their relative abundance, whereas *Sphenolithus*, *Zygrhablithus* and *Octolithus* show a significant decrease in abundance (Figure 4).

[16] Nannofossils constrain the timing of the marly unit at Farra. *Girgisia gammation* is observed almost from the base of the section, whereas *Discoaster multiradiatus* is consistently absent. This suggests that deposition of the lower Eocene sediments began after the extinction of this taxon (Figure 5). The lowest occurrence of *D. lodoensis*, which defines the base of NP12 Zone [*Martini*, 1971], coincides with the base of the marly unit. Consequently, the lower Eocene portion of the Farra section spans the upper part of NP11 through the lower part of NP12 [*Agnini et al.*, 2006b] (Figure 5).

3.3. Planktic Foraminifera and the Siliceous Fraction at Farra

[17] Planktic foraminiferal assemblages are generally abundant and well preserved except for the samples at the base of the marly unit, in which the F index show high values. The distribution of the primary genera also exhibits significant changes. The main feature is a marked abundance increase, up to 90%, of the genus *Acarinina* within the marly unit (Figure 6). This feature starts ~5m below the marly unit, and coincides with an increase in absolute abundance of radiolarians and sponge spicules (Figure 6). The relative abundances of *Subbotina* group and *Morozovella* decrease within the marly unit and gradually recover in its upper part reaching preperturbation values. The first signs of carbonate dissolution are observed below the marly unit as well, in phase with the increase of *Acarinina* (Figure 6).

[18] *Morozovella formosa* and rare, scattered specimens of *M. aragonensis* co-occur from the base of the lower Eocene portion to the top of the section. Thus, the entire section belongs to the E5 Zone of *Berggren and Pearson* [2005]. The biostratigraphic results based on planktic foraminiferal index species are consistent with results obtained using calcareous nannofossil biohorizons.

3.4. Dinocysts at Farra

[19] Approximately half of the samples yield dinocysts, and these generally exhibit rich assemblages. Other samples are barren, likely because of oxidation. The lowermost productive samples, from just below the 0 cm level, are dominated by representatives of *Operculodinium* and *Spiniferites* (Data Set S5), indicating an open marine location of the Farra site during early Eocene times [*Sluijs et al.*, 2005; *Pross and Brinkhuis*, 2005]. At the onset of the negative carbon isotope excursion, however, *Apectodinium* become the dominant constituent and contribute between 20 and 50% of the assemblage in all productive samples within the marly unit (Figure 4). No dinocysts are preserved above the marly unit.

3.5. Benthic Foraminifera at Farra

[20] Benthic foraminifera represent less than 10% of the total foraminiferal content. Calcareous hyaline taxa dominate, representing ca. 80% of the benthic assemblages. No significant changes in the state of preservation of benthic foraminifera have been observed within or across the marly

Figure 3. Correlation between the Farra d'Alpago section, Possagno section, ODP Site 1262, and DSDP Site 577. Calcareous nannofossil biostratigraphy zonation is that of *Martini* [1971]. Magnetostratigraphy and biostratigraphy from Possagno [*Agnini et al.*, 2006b] are plotted with previously unpublished carbon isotope data. The new data from the Possagno section are poorly resolved but provide a reliable marine carbonate $\delta^{13}C$ record in which the PETM and other early Eocene carbon isotope excursions are recognizable. Data from DSDP Site 577 are from *Cramer et al.* [2003] (star). Magnetostratigraphy and biostratigraphy from Walvis Ridge are from *Bowles* [2006] and *Agnini et al.* [2007b] (open circle), whereas MS is from *Zachos et al.* [2004]. The green and orange lines identify the Elmo event and the X event, respectively, and the light red box marks the marly unit. The geomagnetic polarity timescale by *Cande and Kent* [1995] is also provided on the left.

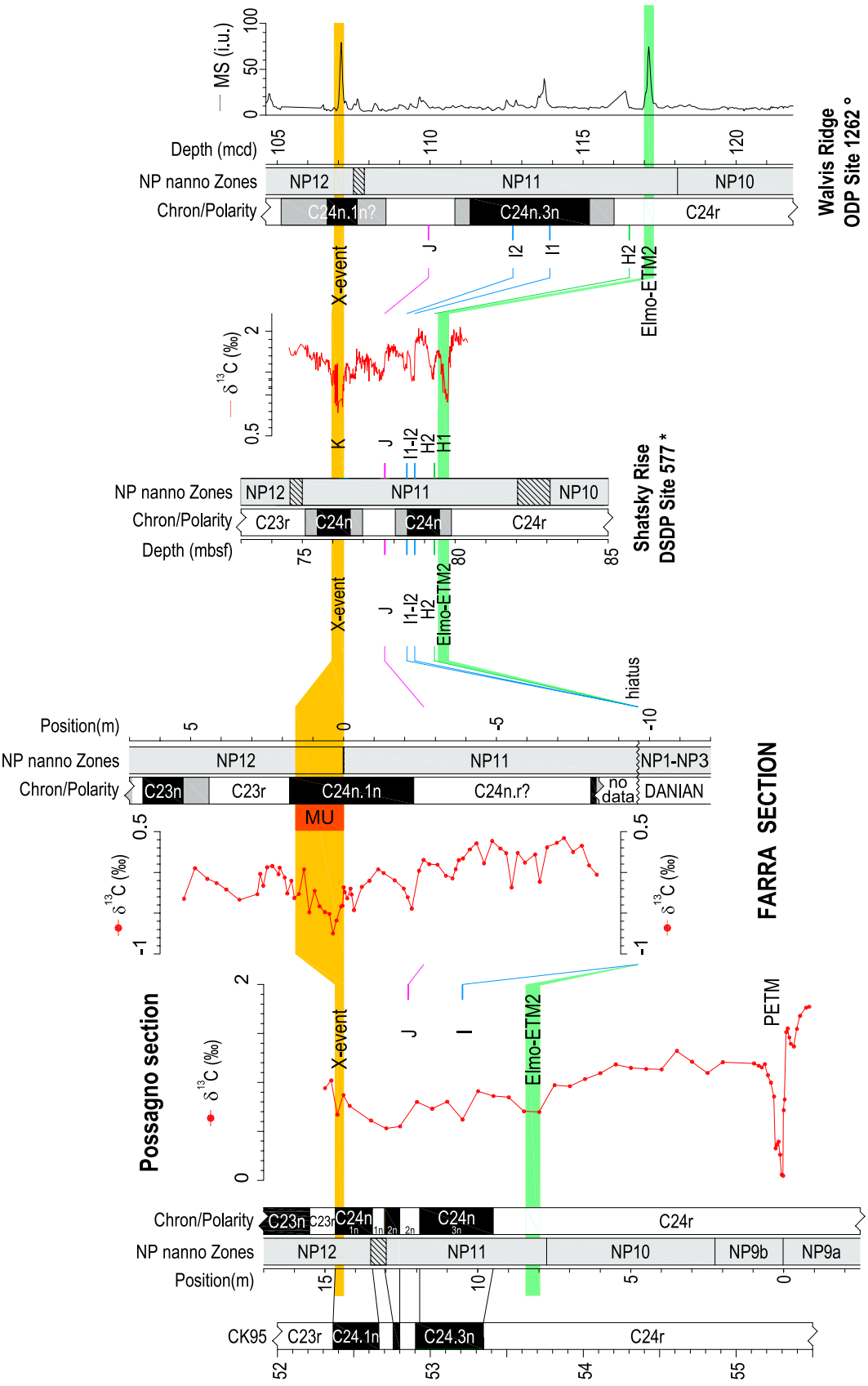
MS (i.u.)
Depth (mcd)
NP nanno Zones
Chron/Polarity
Walvis Ridge
ODP Site 1262 °
X-event
Elmo-ETM2
Shatsky Rise
DSDP Site 577 *
Depth (mbsf)
hiatus
Position(m)
FARRA SECTION
MU
Possagno section
PETM
CK95

Figure 3

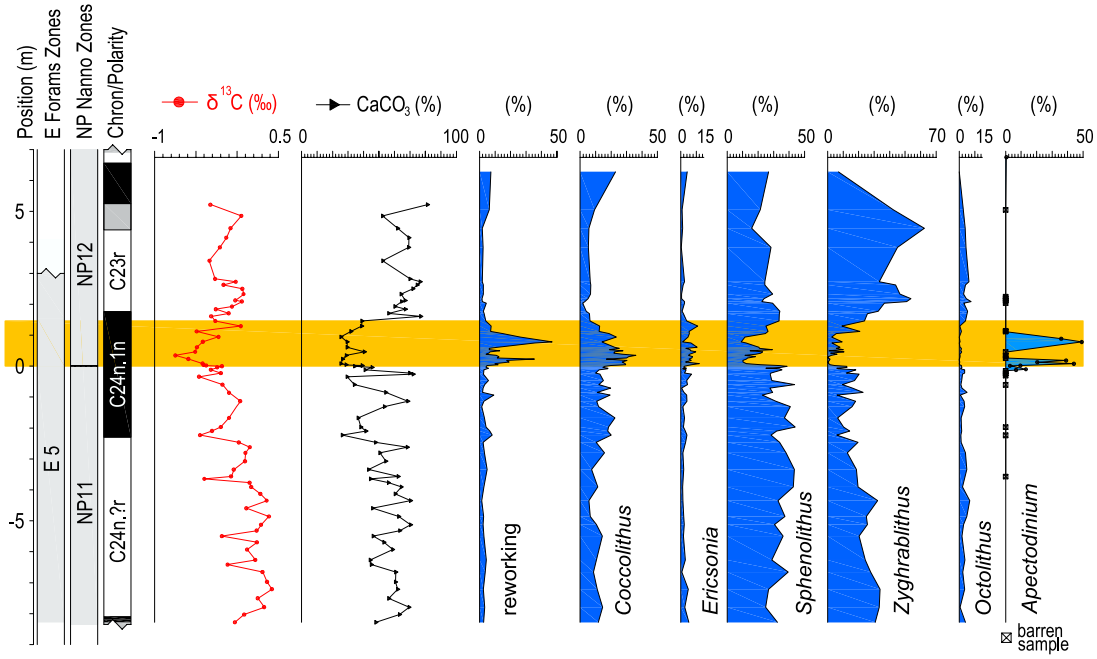

Figure 4. Abundance patterns of selected calcareous nannofossil and dinocyst genera are plotted with $\delta^{13}C$ (‰), $CaCO_3$ content (%), magnetostratigraphy, calcareous nannofossil, and planktic foraminifera biostratigraphy [*Martini*, 1971; *Berggren and Pearson*, 2005]. Gray shaded area represents both the X event and the marly unit.

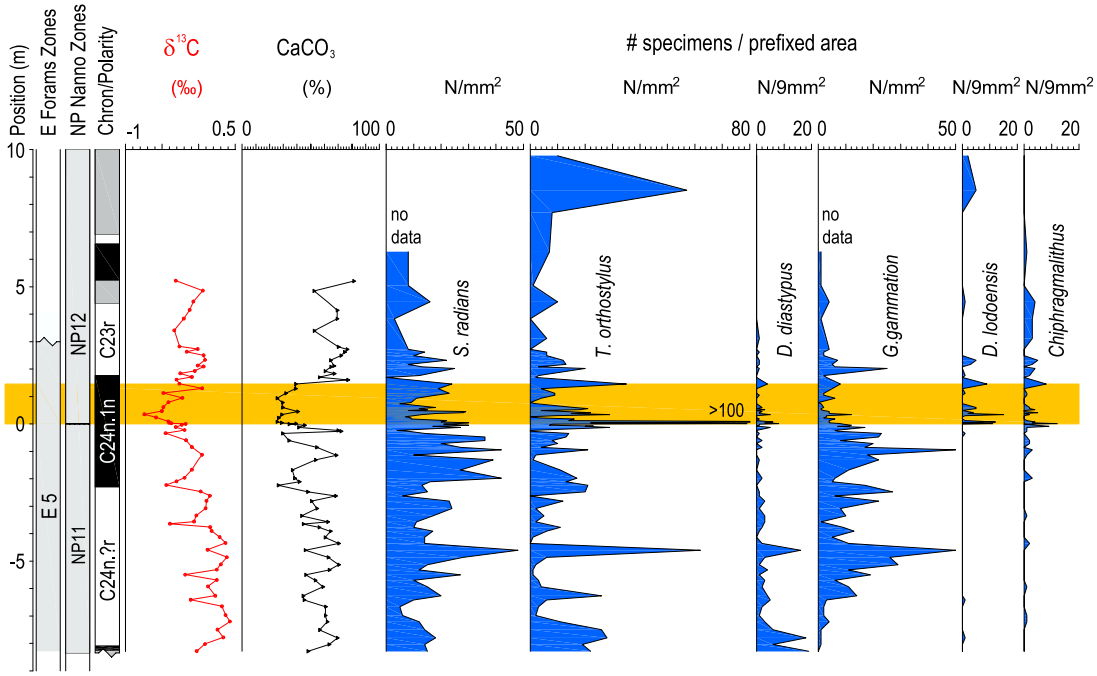

Figure 5. Abundance patterns of selected calcareous nannofossils are plotted with calcareous nannofossil and planktic foraminifera biostratigraphy [*Martini*, 1971; *Berggren and Pearson*, 2005], magnetostratigraphy, $CaCO_3$ content (%), and $\delta^{13}C$ (‰). Gray shaded area represents the X event and the marly unit.

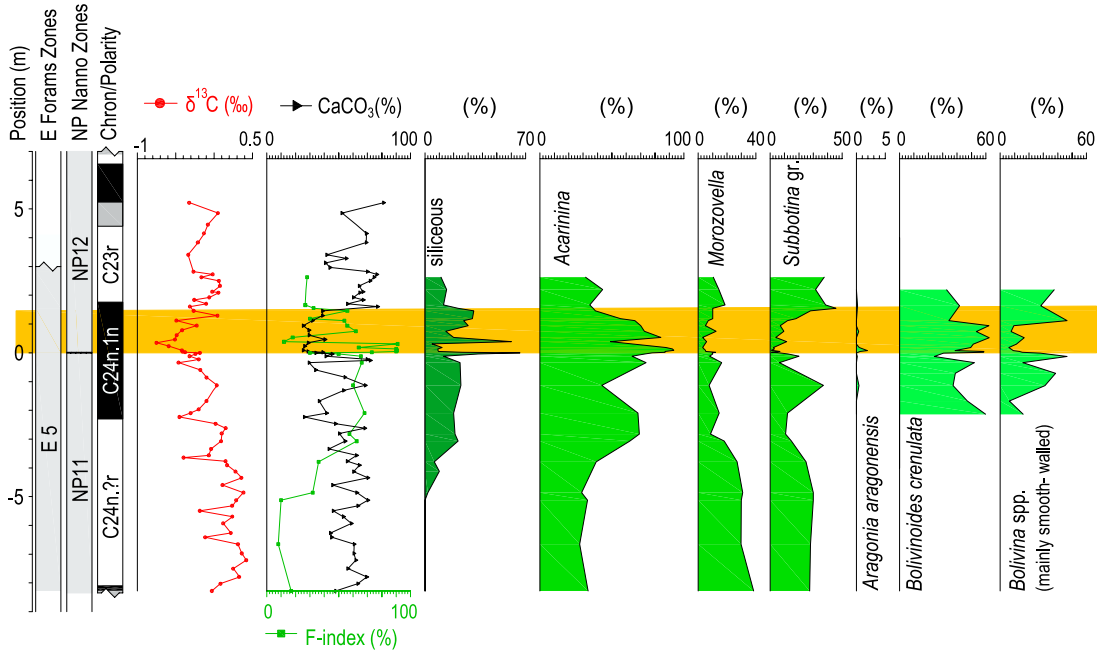

Figure 6. Abundance patterns of selected planktic and benthic foraminiferal taxa are plotted with $\delta^{13}C$ (‰), $CaCO_3$ content (%), magnetostratigraphy, calcareous nannofossil, and planktic foraminifera biostratigraphy [*Martini*, 1971; *Berggren and Pearson*, 2005]. The percentages of the siliceous component and the F index (%) of planktic foraminifera are also provided. The *Subbotina* group includes, besides *Subbotina*, the ecologically similar genera *Parasubbotina* and *Globorotaloides* that, however, constitute a minor component of this group throughout the analyzed interval. Gray shaded area represents both the X event and the marly unit.

unit, except in single sample at its base, which is strongly dissolved. The benthic foraminiferal assemblages are dominated by infaunal morphotypes (Figure 6), specifically Bolivinacea and Buliminacea (biserial and triserial taxa), that are common in assemblages of continental margins [*Thomas*, 2007]. Among Bolivinacea, which in some samples reach 85% of the total assemblage, the most abundant taxa are represented by *Bolivinoides crenulata* and smooth-walled *Bolivina* (Figure 6).

[21] Though scarce, some established paleobathymetric index taxa have been recognized in the assemblages such as *Nuttallides truempyi*, *Oridorsalis umbonatus*, *Bulimina semicostata, Aragonia aragonensis, Cibicidoides eocaenus* and *Anomalinoides capitatus* (Figure 7) [e.g., *Van Morkhoven et al.*, 1986; *Bignot*, 1998; *Ortiz and Thomas*, 2006]. Among these, *Nuttallides truempyi* has an upper depth limit of 500–600 m [*Van Morkhoven et al.*, 1986], but it has been observed also at upper bathyal depths (ca. 300 m) in the Paleocene of Egypt [*Speijer and Schmitz*, 1998].

[22] *Bolivinoides crenulata* has been reported at middle bathyal abyssal paleodepth in late Paleocene-middle Eocene sediments [*Sztrákos*, 2005; *Nomura and Takata*, 2005; *Ortiz and Thomas*, 2006], but its upper depth limit is unknown. *Angulogerina muralis,* a common taxon at Farra, has been considered typical of sublittoral to upper bathyal depths in late Eocene–early Oligocene sediments of Spain [*Molina et al.*, 2006], but it is also common in middle bathyal sediments of Ypresian-Lutetian of Spain [*Ortiz and Thomas*, 2006]. Within agglutinants, *Spiroplectammina navarroana*, *Spiroplectinella subhaeringensis* and *Karrerulina* spp. (*K. horrida* and *K. conversa*) are typical of bathyal abyssal environments [*Kaminski and Gradstein*, 2005]. All these data suggest that the Ypresian sediments of Farra were likely deposited close to the upper middle bathyal boundary (ca. 5–600 m) [*Van Morkhoven et al.*, 1986].

[23] The relative abundance patterns of some taxa as *Nuttalides truempyi, Oridorsalis umbonatus* and the opportunistic *Aragonia aragonensis,* show a slight increase at the base of marly unit (Figure 7) where dissolution of benthic foraminifera is evident. Such increase is less prominent if compared with that observed in early Eocene hyperthermals at ODP Sites 690 and 865 that are located in truly pelagic, much deeper settings [e.g., *Thomas and Shackleton*, 1996; *Thomas*, 1998, 2005, 2007; *Thomas and Zachos*, 2000; *Thomas et al.*, 2006].

3.6. Magnetostratigraphy at Farra

[24] As a rule, a viscous component was eliminated at 200–300°C and a ChRM was isolated in the 200°–300° to 550°–610°C temperature interval (Figures 2a and 2b). Two samples from the base of the section yielded a reverse and normal polarity component in the 300–470°C and 550°–650° temperature intervals, respectively (Figure 2c). We retained the low-temperature component for magnetic stratigraphy, while the high-temperature component (likely carried by hematite) was considered as a normal polarity

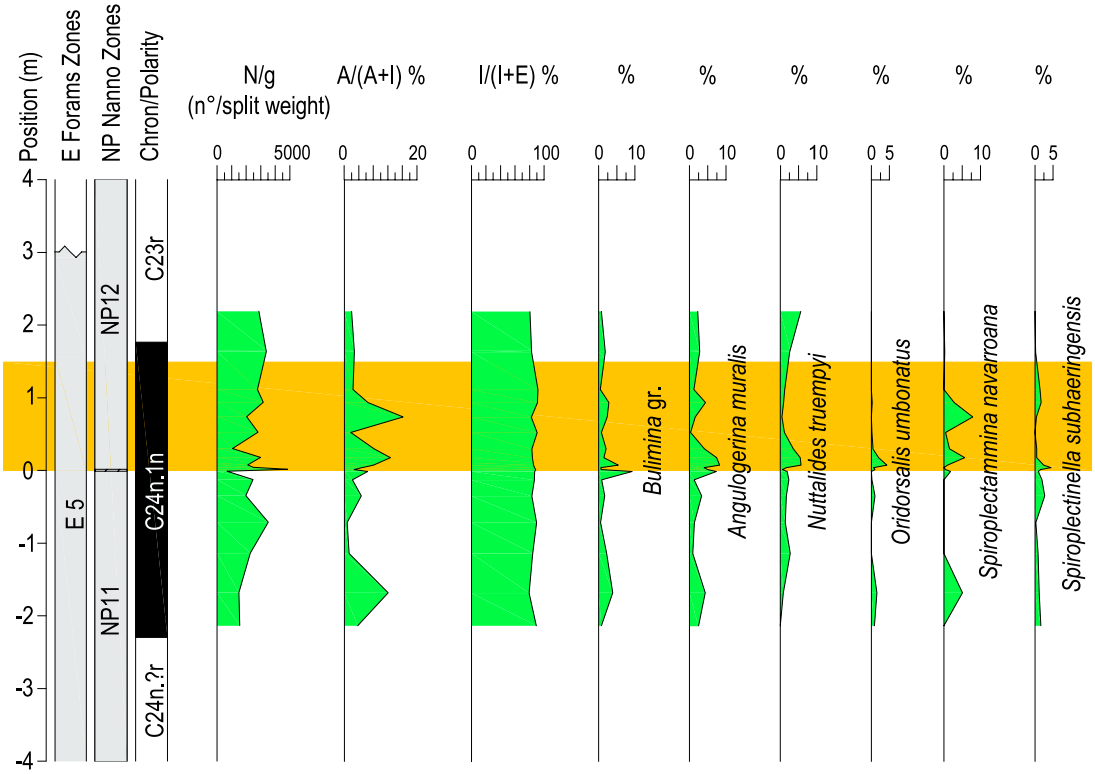

Figure 7. N/g, A/(A+I) (%), and I/(I+E) (%) indexes and the abundance patterns of selected benthic foraminifera are plotted against calcareous nannofossil and planktic foraminifera biostratigraphy [*Martini*, 1971; *Berggren and Pearson*, 2005] and magnetostratigraphy. Gray shaded area represents the X event.

overprint. The individual ChRMs define a succession of normal and reverse polarity magnetozones.

4. Discussion

4.1. Integrated Stratigraphy

[25] Calcareous nannofossil and planktic foraminifera biostratigraphies indicate that the lower Eocene portion of the Farra section spans parts of the NP11–NP12 [*Martini*, 1971] and the E5 biozones [*Berggren and Pearson*, 2005]. The base of the marly unit nearly coincides with the base of NP12. The NP11/12 boundary falls within an interval of normal polarity in the Farra section as well as, for example, at ODP Site 1262 and DSDP Site 550 (Figure 3) [*Cramer et al.*, 2003]. The negative carbon isotope excursion occurs within the upper part of this interval of normal polarity. An interval of reversed polarity in the Farra section, within Zone NP11, is underlain by an interval of normal polarity, still within Zone NP11 (Figure 3). As previously observed, the NP11 Zone encompasses the interval from uppermost polarity chron C24r to at least the mid part of chron C24n [*Berggren et al.*, 1995; *Cramer et al.*, 2003; *Agnini et al.*, 2007b]. All these data imply that the interval of normal polarity straddling the NP11/12 boundary represents subchron C24n.1n. Hence, the sequence of normal and reverse polarity intervals, progressively numbered starting from the Farra section bottom (Figure 2e), can be correlated with the geomagnetic polarity timescale of *Cande and Kent* [1995] and has been used to tie the observed magnetozones with polarity chrons (Figures 2e and 3).

4.2. Position of the X Event and Global Correlations

[26] Several negative carbon isotope shifts, including ETM2 and X, occur during the early Eocene. *Cramer et al.* [2003] have identified at least six events (i.e., H1, H2, I1 I2, J, and K) in the Pacific and Atlantic Oceans between the upper part of chron C24r and chron C24n. Several of these events have been also found and clearly correlated in South Atlantic, the Arctic Ocean and New Zealand [*Zachos et al.*, 2004; *Nicolo et al.*, 2007; *Sluijs et al.*, 2008a] and perhaps in the North Sea [*Sluijs et al.*, 2008b]. Here, we compare our data to those reported from North Pacific Site 577 and South Atlantic Site 1262 in order to trace the X (K) event over wide areas (Figure 3).

[27] The H1 and K events observed at Site 577 are clearly correlative to the Elmo and X events both at Site 1262 [*Lourens et al.*, 2005; *Röhl et al.*, 2004] and in the Possagno section (Figure 3). In addition, the X event is also correlative with the negative carbon shift recorded in the Farra section. Moreover, these minor events recorded in the Pacific (e.g., the H1, H2, I1, I2) are correlated with magnetic susceptibility (MS) spikes at Site 1262 [see *Nicolo et al.*, 2007], because of the lacking of an accurate carbon and oxygen isotopes record at this site. Following these authors we use the same proxy to correlate the two uppermost events, that are the J and the X (K) events (Figure 3). Unfortunately,

these minor multiple $\delta^{13}C$ excursions, clearly recognized in other sections, are missing or hinge on a single datum in the Possagno section. Nevertheless, the presence of several more marly intervals lying between 8 and 14 m level could well represent all these minor phases, because the biomagnetostratigraphic framework from Possagno indicate that this section is complete at least within the available biomagnetostratigraphic resolution.

[28] The stratigraphic correlation between ODP/DSDP Sites and our Tethyan sections suggests that the marly unit, deposited during the X event, represents the local expression of a global event that can be documented over wide areas in the Pacific and Atlantic oceans. Moreover, the age models developed for the Farra and Possagno sections indicate a precise biomagnetostratigraphic position, within subchron C24n.1n, thus providing an accurate chronological framework for the X event.

4.3. Biotic Response to Environmental Changes

[29] Hitherto, we have demonstrated that the Farra section holds an expanded record of the X event and is thus well suited for a detailed study of the response of calcareous plankton, in a deep water, albeit near-continental, hemipelagic setting. The prominent modifications in our biotic records must reflect significant environmental changes in the Tethyan realm. At some intervals, however, paleoenvironmental reconstructions are limited by preservational issues, such as carbonate dissolution and organic matter oxidation.

4.3.1. Calcareous Nannofossils

[30] Over the past 30 years, several studies of calcareous nannofossils have provided a strong basis for interpreting assemblages as a proxy of paleoceanographic changes [e.g., *Haq and Lohmann*, 1976; *Wei and Wise*, 1990; *Aubry*, 1998; *Bralower*, 2002]. During the X event, the calcareous nannofossil assemblages are characterized by an increase of obviously reworked specimens, *Coccolithus pelagicus* and *Ericsonia* [*Wei and Wise*, 1990; *Kelly et al.*, 1996; *Monechi et al.*, 2000; *Bralower*, 2002; *Agnini et al.*, 2007a], and a concomitant decrease of taxa considered to reflect oligotrophic conditions such as *Sphenolithus*, *Zygrhablithus,* and *Octolithus* [*Haq and Lohmann*, 1976; *Aubry*, 1998; *Bralower*, 2002; *Gibbs et al.*, 2004, 2006; *Agnini et al.*, 2007a] (Figure 4). Similar changes in assemblage abundances have been observed from sediments documenting the PETM event in this region of the western central Tethys [*Agnini et al.*, 2007a]. The relative increase in warm eutrophic taxa coupled with the marked decrease of taxa thriving in oligotrophic conditions suggests transient enrichment in dissolved nutrients in warmer sea surface waters.

[31] The increase in reworked Cretaceous forms may indicate a huge increase in terrigenous input, which was likely produced by the chemical weathering accelerated by the enhanced hydrological cycle, as recorded also for the PETM [*Ravizza et al.*, 2001; *Schmitz et al.*, 2001; *Crouch et al.*, 2003; *Hollis et al.*, 2005; *Zachos et al.*, 2005; *Giusberti et al.*, 2007; *Nicolo et al.*, 2007; *Sluijs et al.*, 2008a, 2008b]. Specifically, the rocks in the Farra section represent a variable mixture of allochemic and terrigenous sediments. Allochemic sediments consist of precipitated nondetrital carbonate fragments (allochems) that undergo a brief history of transport and abrasion prior to deposition, whereas terrigenous sediments are produced by the weathering of preexisting rocks, siliciclastic and carbonate, and the subsequent transportation and deposition of the weathering products. The enhanced weathering, often invoked for the hyperthermals, likely affects siliciclastic as well as carbonate rocks and thus produces a significant increase of the detrital component.

4.3.2. Planktic Foraminifera

[32] Life strategies of early Paleogene planktic foraminiferal taxa have been thoroughly investigated over the past 30–40 years. These strategies are thought to be highly useful for reconstruction of paleoenvironmental conditions [*Douglas and Savin*, 1978; *Boersma et al.*, 1979, 1987; *Shackleton et al.*, 1985; *Bralower et al.*, 1995; *Lu and Keller*, 1996; *Luciani et al.*, 2007]. Fluctuations in composition and abundance among planktic foraminiferal assemblages during the K event include a pronounced increase of the warm water indicator *Acarinina*, a concomitant strong reduction of the cold water indicator *Subbotina* (group) and a marked reduction of the highly specialized warm oligotrophic *Morozovella* [*Pearson et al.*, 2006]. A realistic reconstruction of the paleoenvironmental conditions can thus be obtained using paleoecological affinity, trophic strategies and changes in depth-related specializations in planktic foraminiferal taxa. In particular, late Paleocene and early Eocene $\delta^{13}C$ and $\delta^{18}O$ data from locations with a shallow mixed layer and strong thermal gradients show slight differences between isotope values measured on *Acarinina* and *Morozovella*, with heavier $\delta^{18}O$ and lighter $\delta^{13}C$ values in *Acarinina* than in *Morozovella*. This suggests that representatives of the genus *Acarinina* may have grown in deeper and more nutrient-rich waters compared with contemporaneous *Morozovella* [*Bralower et al.*, 1995; *Quillévéré et al.*, 2001; *Quillévéré and Norris*, 2003]. It follows that, during the K event at Farra, the surface dwelling acarininids were able to temporarily colonize warmer deeper and nutrient-richer waters previously occupied by *Subbotina* and better tolerate the relatively high eutrophic conditions which prevented the genus *Morozovella* to thrive. This scenario is consistent with a rapid warming and enhanced eutrophic conditions. The temporary but profound modifications in the planktic foraminiferal assemblages strongly resemble those observed in a similar environmental setting from the Belluno Basin across the PETM [*Luciani et al.*, 2007].

4.3.3. Dinocysts

[33] The dinoflagellate response to the X event consists of an acme of the tropical genus *Apectodinium* that also characterizes numerous PETM sections worldwide [*Bujak and Brinkhuis*, 1998; *Sluijs et al.*, 2007a]. The peridinioid *Apectodinium* likely represents a heterotrophic dinoflagellate [*Bujak and Brinkhuis*, 1998; *Crouch et al.*, 2001], whose proliferation occurs in high-SST conditions, but is eventually favored by stratification of the water column, high-nutrient loads and/or abundant prey [*Sluijs et al.*, 2007b, 2008a].

4.3.4. Benthic Foraminifera

[34] The domination of infaunal morphogroups such as Buliminacea and Bolivinacea within and across the MU at

Farra has been interpreted, following *Thomas* [2007], as an indicator of abundant food conditions on the seafloor (Figure 6). The marked increase in terrigenous input observed within the marly unit coincides with a temporary crossover in abundance between *B. crenulata* and *Bolivina*. This change in the benthic foraminiferal assemblages may indicate that *B. crenulata* was better adapted than *Bolivina* to the stressed conditions that characterize the X event (Figure 6).

4.3.5. Eutrophication During the X Event at Farra

[35] The significant fluctuations in calcareous nannofossil and planktic foraminiferal assemblages and the marked increase in *Apectodinium* are thus consistent with the often invoked hypothesis of increased runoff and nutrient delivery to the oceans during hyperthermal times [*Schmitz et al.*, 2001; *Crouch et al.*, 2003; *Pagani et al.*, 2006; *Zachos et al.*, 2006; *Giusberti et al.*, 2007; *Schmitz and Pujalte*, 2007; *Nicolo et al.*, 2007; *Sluijs et al.*, 2008b]. The X event is characterized by a series of biological and geochemical signals, which include, for example, a transient, perturbation of the marine biota and a prominent negative excursion in both $\delta^{13}C$ and $\delta^{18}O$ isotopes. These signatures are virtually identical, although smaller in amplitude and shorter in duration, to those observed during the PETM event from the neighboring Forada section [*Giusberti et al.*, 2007; *Agnini et al.*, 2007a; *Luciani et al.*, 2007], or from most other marine PETM sections worldwide [*Schmitz et al.*, 2001; *Crouch et al.*, 2003; *Zachos et al.*, 2006]. One of the existing productivity models during the PETM infers high-productivity conditions on shelf/slope areas and increased oligotrophic conditions in open ocean sites [*Gibbs et al.*, 2006]. Likewise, the increased nutrient availability inferred from the Farra hemipelagic section during the X event may be explained by an increased content of nutrients not only in the shelf, but also in hemipelagic settings, and a possible decoupling between eutrophic shelf/slope environments and oligotrophic pelagic areas. Actually, a larger data set from truly pelagic and shelf/slope areas is needed to reconstruct a more comprehensive scenario supporting or discarding this hypothesis.

[36] Despite of these broad similarities, the PETM produced global, though transient, changes in the planktic biota, i.e., short-lived odd forms [*Aubry et al.*, 2002; *Kelly et al.*, 1996; *Bowen et al.*, 2006; *Sluijs et al.*, 2007a], whereas the biotic responses to the perturbation occurring during the X event, especially for calcareous plankton, are restricted to sharp changes in the relative abundance of taxa likely related to short-lived modifications in the local environmental conditions. The X event is not characterized by the presence of the so-called calcareous plankton excursion taxa, as is the case of the PETM. This may suggest that a threshold in the photic zone ocean chemistry has to be passed to produce malformations and/or short-lived taxa that are better adapted to survive briefly during short periods of extreme paleoenvironmental conditions. This threshold was not passed when the input of light carbon to the biosphere produced a global negative carbon isotope excursion of ~0.6‰ during the X event, but was passed when the input generated an excursion on the order of about 3‰ during the PETM.

5. Hyperthermal Events or Regime During the Early Eocene?

[37] The global extent of short-lived carbon cycle perturbations in the early Eocene has been documented both in deep-sea, hemipelagic and shelf settings [*Cramer et al.*, 2003; *Nicolo et al.*, 2007; *Sluijs et al.*, 2008b]. The coupled decrease in $\delta^{13}C$ and $\delta^{18}O$ values, the decrease in $CaCO_3$, produced by dissolution and/or dilution of biogenic carbonate, and transient biotic changes characterize these perturbations. Repeated occurrences of these short-lived events during the early Paleogene have been interpreted to be paced by Milankovitch cycles [*Cramer et al.*, 2003; *Lourens et al.*, 2005; *Westerhold et al.*, 2007]. If this is the case, the orbital pacing eventually controls the timing and, perchance, the intensity of these phases. Astronomically tuned expanded successions spanning the early Paleogene must be analyzed in order to test this hypothesis. Unfortunately, though the Farra section has a good chronologic control, only the X (K) and J events are preserved and the section is thus not ideally suitable to add pieces of evidence to support or refute this hypothesis.

[38] Although many characters in the post-PETM hyperthermal events are similar to those characterizing the PETM event, they are all less intense and of shorter duration [*Lourens et al.*, 2005; *Nicolo et al.*, 2007; *Stap et al.*, 2009]. They also show a more rapid recovery to preevent conditions compared to the duration of the PETM recovery interval [*Quillévéré et al.*, 2008]. Some authors hypothesize that the early Eocene hyperthermals result from repeated releases of methane hydrates, possibly uncorked by precursor deep-sea warmings [*Nicolo et al.*, 2007; *Sluijs et al.*, 2007b]. In contrast, *Quillévéré et al.* [2008] suggest that the repeated occurrences of negative excursions of $\delta^{13}C$, their modest size and rapid rate of recovery, indicate that the carbon is not originating from deeply buried sources, but rather represent redistribution of carbon within the biosphere. Thus, although the trigger mechanism(s) of these post-PETM hyperthermal events remains debated, they appear to be globally recognizable and certainly represent peculiar features of short duration that repeatedly interrupted the longer-term evolution of Paleocene and early Eocene paleoclimates.

6. Conclusions

[39] We present data from a new section in the Venetian pre-Alps containing a carbon cycle perturbation that is correlated to the early Eocene K event of *Cramer et al.* [2003], which corresponds to the X event of *Zachos et al.* [2004]. The X event in the Farra section is characterized by a negative carbon isotope excursion in bulk carbonate of 0.6‰, carbonate dissolution at its base, PETM-like responses in calcareous nannofossils, foraminifera and dinocyst and an increase in terrestrial run off. Although the X event shows a smaller magnitude changes that the PETM and ETM2 (Elmo event), all these events show

strong similarities in their geochemical and biotic features. Our age model places this event within subchron C24n.1n at about 52.5 Ma, when adopting the timescale of *Cande and Kent* [1995]. The X event is one of several events driven by shifts in the global carbon pool during the early Eocene, producing large changes in ocean chemistry and profound modifications in marine biota. An additional interesting characteristic, indicated by the planktic foraminiferal record, is that a marked environmental instability started well before the onset of the negative $\delta^{13}C$ excursion, thus preceding the main perturbation affecting the geobiosphere.

[40] Even if the X event was less intense than the PETM, judging from, for example, the magnitude of the carbon isotope excursion, the X event represents an abrupt and short-lived episode of global perturbation that resulted in eutrophication of the sea surface waters, at least in the deep-sea, near-continental setting represented by the Farra section in the Tethys. If taken into account that the X event has been recognized also from the midlatitude NE Atlantic, the subtropical NW Atlantic and the tropical NW Pacific oceans [*Cramer et al.*, 2003], it appears reasonable to assume that this event is global in character.

[41] **Acknowledgments.** C.A., E.F., L.G., V.L., and D.R. were supported by MIUR-PRIN grant 2005044839_004. V.L. was also supported by Ferrara University. Financial support was provided by the INGV to P.M. and F.S. J.B. was supported by Stockholm University and VR. Funding for this research was provided to H.B. and A.S. by the ALW-NWO through VENI grant 863.07.001 to A.S. We are grateful to Gerald Dickens, Frédéric Quillévéré, and Ellen Thomas for thorough and constructive reviews of the original manuscript, as we are to Simone Galeotti and Ursula Röhl for fruitful discussions.

References

Agnini, C., E. Fornaciari, L. Giusberti, J. Backman, P. Grandesso, V. Luciani, D. Scardanzan, and D. Rio (2006a), In search of early Eocene hyperthermals: The Farra d'Alpago section (Southern Alps, Italy), in *Climate and Biota of the Early Paleogene 2006*, abstract volume, edited by F. Caballero et al., p. 2, Croman, Bilbao, Spain.

Agnini, C., G. Muttoni, D. V. Kent, and D. Rio (2006b), Eocene biostratigraphy and magnetic stratigraphy from Possagno, Italy: The calcareous nannofossil response to climate variability, *Earth Planet. Sci. Lett.*, *241*, 815–830, doi:10.1016/j.epsl.2005.11.005.

Agnini, C., E. Fornaciari, D. Rio, F. Tateo, J. Backman, and L. Giusberti (2007a), Responses of calcareous nannofossil assemblages, mineralogy and geochemistry to the environmental perturbations across the Paleocene/Eocene boundary in the Venetian pre-Alps, *Mar. Micropaleontol.*, *63*, 19–38, doi:10.1016/j.marmicro.2006.10.002.

Agnini, C., E. Fornaciari, I. Raffi, D. Rio, U. Röhl, and T. Westerhold (2007b), High-resolution nannofossil biochronology of middle Paleocene to early Eocene at ODP Site 1262: Implications for calcareous nannoplankton evolution, *Mar. Micropaleontol.*, *64*, 215–248, doi:10.1016/j.marmicro.2007.05.003.

Alegret, L., E. Molina, and E. Thomas (2003), Benthic foraminiferal turnover across the Cretaceous/Paleogene boundary at Agost (southeastern Spain): Paleoenvironmental inferences, *Mar. Micropaleontol.*, *48*, 251–279, doi:10.1016/S0377-8398(03)00022-7.

Arenillas, I., E. Molina, and B. Schmitz (1999), Planktic foraminiferal and ^{13}C isotopic changes across the Paleocene/Eocene boundary at Possagno (Italy), *Int. J. Earth Sci.*, *88*(2), 352–364, doi:10.1007/s005310050270.

Aubry, M.-P. (1984), *Handbook of Cenozoic Calcareous Nannoplankton, vol. 1, Ortholithae (Discoaster)*, 263 pp., Micropaleontology, Am. Mus. of Nat. Hist., New York.

Aubry, M.-P. (1988), *Handbook of Cenozoic Calcareous Nannoplankton, vol. 2, Ortholithae (Holococcoliths, Ceratoliths, Ortholiths and Other)*, 279 pp., Micropaleontology, Am. Mus. of Nat. Hist., New York.

Aubry, M.-P. (1989), *Handbook of Cenozoic Calcareous Nannoplankton, vol. 3, Ortholithae (Pentaliths and Others), Heliolithae (Fasciculiths, Sphenoliths and Others)*, 279 pp., Micropaleontology, Am. Mus. of Nat. Hist., New York.

Aubry, M.-P. (1990), *Handbook of Cenozoic Calcareous Nannoplankton, vol. 4, Heliolithae (Helicoliths, Cribriliths, Lopadoliths and Other)*, 381 pp., Micropaleontology, Am. Mus. of Nat. Hist., New York.

Aubry, M.-P. (1998), Early Paleogene calcareous nannoplankton evolution: A tale of climatic amelioration, in *Late Paleocene and Early Eocene Climatic and Biotic Evolution*, edited by M.-P. Aubry et al., pp. 158–203, Columbia Univ. Press, New York.

Aubry, M.-P. (1999), *Handbook of Cenozoic Calcareous Nannoplankton, vol. 5, Heliolithae (Zygoliths and Rhabdoliths)*, 368 pp., Micropaleontology, Am. Mus. of Nat. Hist., New York.

Aubry, M.-P., K. Ouda, C. Dupuis, J. A. Van Couvering, and the members of the Working Group on the Paleocene/Eocene Boundary (2002), Proposal: Global standard stratotype-section and point (GSSP) at the Dababiya section (Egypt), internal report, 58 pp., Int. Subcomm. on Paleogene Stratigr., Trondheim, Norway.

Backman, J., and N. J. Shackleton (1983), Quantitative biochronology of Pliocene and early Pleistocene calcareous nannoplankton from the Atlantic, Indian and Pacific Oceans, *Mar. Micropaleontol.*, *8*, 141–170, doi:10.1016/0377-8398(83)90009-9.

Berggren, W. A., and P. N. Pearson (2005), A revised tropical to subtropical Paleogene planktonic foraminiferal zonation, *J. Foraminiferal Res.*, *35*, 279–298, doi:10.2113/35.4.279.

Berggren, W. A., D. V. Kent, C. C. Swisher III, and M.-P. Aubry (1995), A revised Cenozoic geochronology and chronostratigraphy, in *Geochronology, Time Scales, and Global Stratigraphic Correlation*, edited by W. A. Berggren et al., *Spec. Publ. SEPM Soc. Sediment. Geol.*, vol. 54, pp. 129–212.

Bignot, G. (1998), Middle Eocene benthic foraminifers from holes 960A and 960C, central Atlantic Ocean, *Proc. Ocean Drill. Program Initial Rep.*, *208*, 433–444.

Boersma, A., N. J. Shackleton, M. Hall, and Q. Given (1979), Carbon and oxygen isotope records at DSDP Site 384 (North Atlantic) and some Paleocene paleotemperatures and carbon isotope variations in the Atlantic Ocean, *Initial Rep. Deep Sea Drill. Proj.*, *43*, 695–717.

Boersma, A., I. P. Silva, and N. J. Shackleton (1987), Atlantic Eocene planktonic foraminiferal paleohydrographic indicators and stable isotope paleoceanography, *Paleoceanography*, *2, 287–331, doi:10.1029/PA002i003p00287.*

Bolli, H. M., (1975), *Monografia Micropaleontologica sul Paleocene e l'Eocene di Possagno, Provincia di Treviso, Italia*, *Schweiz. Palaeontol. Abh., 97*, 222 pp.

Bowen, G. J., et al. (2006), Eocene hyperthermal event offers insight into greenhouse warming, *Eos Trans. AGU*, *87*(17), doi:10.1029/2006EO170002.

Bowles, J. (2006), Data report: Revised magnetostratigraphy and magnetic mineralogy of sediments from Walvis Ridge, Leg 208, *Proc. Ocean Drill. Program Sci. Results*, *208*, 1–24.

Bralower, T. J. (2002), Evidence of surface water oligotrophy during the Paleocene-Eocene thermal maximum: Nannofossil assemblage data from Ocean Drilling Program Site 690, Maud Rise, Weddell Sea, *Paleoceanography*, *17*(2), 1023, doi:10.1029/2001PA000662.

Bralower, T. J., J. C. Zachos, E. Thomas, M. Parrow, C. K. Paull, D. C. Kelly, I. P. Silva, W. V. Sliter, and K. C. Lohmann (1995), Late Paleocene to Eocene paleoceanography of the equatorial Pacific Ocean: Stable isotopes recorded at Ocean Drilling Program Site 865, Allison Guyot, *Paleoceanography*, *10*, 841–865, doi:10.1029/95PA01143.

Bralower, T. J., et al. (2002), *Proceedings of the Ocean Drilling Program Initial Reports*, vol. 198, doi:10.2973/odp.proc.ir.198.2002, Ocean Drill. Program, College Station, Tex.

Bujak, J. P., and H. Brinkhuis (1998), Global warming and dinocyst changes across the Paleocene/Eocene epoch boundary, in *Late Paleocene–Early Eocene Biotic and Climatic Events in the Marine and Terrestrial Records*, edited by M.-P. Aubry et al., pp. 277–295, Columbia Univ. Press, New York.

Cande, S. C., and D. V. Kent (1995), Revised calibration of the geomagnetic polarity timescale for the Late Cretaceous and Cenozoic, *J. Geophys. Res.*, *100*(B4), 6093–6096, doi:10.1029/94JB03098.

Cati, A., D. Sartorio, and S. Venturini (1989), Carbonate platforms in the subsurface of the northern Adriatic area, *Mem. Soc. Geol. Ital.*, *40*, 295–308.

Coccioni, R., E. Angori, R. Catanzariti, L. Giusberti, E. Guasti, V. Luciani, A. Marsili, S. Monechi, M. Sprovieri, and F. Tateo (2006), The early Paleogene hyperthermal events (EPHES):

New insights from the classical tethyan Contessa Road section (Gubbio, Italy), in *Climate and Biota of the Early Paleogene 2006*, abstract volume, edited by F. Caballero et al., p. 27, Croman, Bilbao, Spain.

Cramer, B. S., J. D. Wright, D. V. Kent, and M.-P. Aubry (2003), Orbital climate forcing of $\delta^{13}C$ excursions in the late Paleocene–early Eocene (chrons C24n–C25n), *Paleoceanography*, *18*(4), 1097, doi:10.1029/2003PA000909.

Crouch, E. M., C. Heilmann-Clausen, H. Brinkhuis, H. E. G. Morgans, K. M. Rogers, H. Egger, and B. Schmitz (2001), Global dinoflagellate event associated with the late Paleocene thermal maximum, *Geology*, *29*(4), 315–318, doi:10.1130/0091-7613(2001)029<0315:GDEAWT>2.0.CO;2.

Crouch, E. M., G. R. Dickens, H. Brinkhuis, M.-P. Aubry, G. J. Hollis, K. M. Rogers, and H. Visscher (2003), The Apectodinium acme and terrestrial discharge during the Paleocene-Eocene thermal maximum: New palynological, geochemical and calcareous nannoplankton observations at Tawanui, New Zealand, *Palaeogeogr. Palaeoclimatol. Palaeoecol.*, *194*, 387–403, doi:10.1016/S0031-0182(03)00334-1.

Denman, K. L., et al. (2007), Couplings between changes in the climate system and biogeochemistry, in *Climate Change 2007: The Physical Science Basis: Working Group I Contribution to the Fourth Assessment Report of the IPCC*, edited by S. Solomon et al., pp. 499–588, Cambridge Univ. Press, New York.

Dickens, G. R., J. R. O'Neil, D. K. Rea, and R. M. Owen (1995), Dissociation of oceanic methane hydrate as a cause of the carbon isotope excursion at the end of the Paleocene, *Paleoceanography*, *10*, 965–971, doi:10.1029/95PA02087.

Dickens, G. R., M. M. Castillo, and J. C. G. Walker (1997), A blast of gas in the latest Paleocene: Simulating first-order effects of massive dissociation of oceanic methane hydrate, *Geology*, *25*(3), 259–262, doi:10.1130/0091-7613(1997)025<0259:ABOGIT>2.3.CO;2.

Douglas, R. G., and S. M. Savin (1978), Oxygen isotopic evidence for the depth stratification of Tertiary and Cretaceous planktic foraminifera, *Mar. Micropaleontol.*, *3*, 175–196, doi:10.1016/0377-8398(78)90004-X.

Fensome, R. A., and G. L. Williams (2004), *The Lentin and Williams Index of Fossil Dinoflagellates: 2004 Edition*, *Contrib. Ser.*, vol. 42, 909 pp., Am. Assoc. of Stratigr. Palynol., Pittsburgh, Pa.

Fisher, R. (1953), Dispersion on a sphere, *Proc. R. Soc. London, Ser. A*, *217*, 295–305, doi:10.1098/rspa.1953.0064.

Gibbs, S. J., N. J. Shackleton, and J. R. Young (2004), Orbitally forced climate signals in mid-Pliocene nannofossil assemblages, *Mar. Micropaleontol.*, *51*, 39–56, doi:10.1016/j.marmicro.2003.09.002.

Gibbs, S. J., T. J. Bralower, P. R. Bown, J. C. Zachos, and L. M. Bybell (2006), Shelf and open-ocean calcareous phytoplankton assemblages across the Paleocene–Eocene thermal maximum: Implications for global productivity gradients, *Geology*, *34*(4), 233–236, doi:10.1130/G22381.1.

Giusberti, L., D. Rio, C. Agnini, J. Backman, E. Fornaciari, F. Tateo, and M. Oddone (2007), Mode and tempo of the Paleocene Eocene thermal maximum in an expanded section from the Venetian pre-Alps, *Geol. Soc. Am. Bull.*, *119*, 391–412, doi:10.1130/B25994.1.

Hancock, H. J. L., and G. R. Dickens (2005), Carbonate dissolution episodes in Paleocene and Eocene sediment, Shatsky Rise, west-central Pacific [online], *Proc. Ocean Drill. Program Sci. Results, 198*, 24 pp. (Available at http://www-odp.tamu.edu/publications/198_SR/116/116.htm)

Haq, B. U., and G. P. Lohmann (1976), Early Cenozoic calcareous nannoplankton biogeography of the Atlantic Ocean, *Mar. Micropaleontol.*, *1*, 119–194, doi:10.1016/0377-8398(76)90008-6.

Hollis, C. J., G. R. Dickens, B. D. Field, C. M. Jones, and C. P. Strong (2005), The Paleocene-Eocene transition at Mead Stream, New Zealand: A southern Pacific record of early Cenozoic global change, *Palaeogeogr. Palaeoclimatol. Palaeoecol.*, *215*, 313–343, doi:10.1016/j.palaeo.2004.09.011.

Istituto Nazionale di Geofisica e Vulcanologia (2007), Italian magnetic network and geomagnetic field maps of Italy at year 2005.0, *Boll. Geod. Sci. Affini.*, *65*, 1–47.

Jansen, E., et al. (2007), Palaeoclimate, in *Climate Change 2007: The Physical Science Basis: Working Group I Contribution to the Fourth Assessment Report of the IPCC*, edited by S. Solomon et al., pp. 435–498, Cambridge Univ. Press, New York.

Kaminski, M. A., and F. M. Gradstein (2005), *Atlas of Paleogene Cosmopolitan Deep-Water Agglutinated Foraminifera*, *Spec. Publ.*, vol. 10, 548 pp., Grzybowski Found., Krakow, Poland.

Kelly, D. C., T. J. Bralower, J. C. Zachos, I. Premoli Silva, and E. Thomas (1996), Rapid diversification of planktonic foraminifera in the tropical Pacific (ODP Site 865) during the late Paleocene thermal maximum, *Geology*, *24*(5), 423–426, doi:10.1130/0091-7613(1996)024<0423:RDOPFI>2.3.CO;2.

Kennett, J. P., and L. D. Stott (1991), Abrupt deep-sea warming, palaeoceanographic changes and benthic extinctions at the end of the Palaeocene, *Nature*, *353*, 225–229, doi:10.1038/353225a0.

Kirschvink, J. L. (1980), The least squares line and plane and the analysis of paleomagnetic data, *Geophys. J. R. Astron. Soc.*, *62*, 699–718.

Kleypas, J. A., R. A. Feely, V. J. Fabry, C. Langdon, C. L. Sabine, and L. L. Robbins (2006), Impacts of ocean acidification on coral reefs and other marine calcifiers: A guide for future research, report, 88 pp., NSF, Arlington, Va.

Lirer, F. (2000), A new technique for retrieving calcareous microfossils from lithified lime deposits, *Micropaleontology*, *46*, 365–369.

Lourens, L. J., A. Sluijs, D. Kroon, J. C. Zachos, E. Thomas, U. Röhl, J. Bowles, and I. Raffi (2005), Astronomical pacing of late Palaeocene to early Eocene global warming events, *Nature*, *435*, 1083–1087, doi:10.1038/nature03814.

Lu, G., and G. Keller (1996), Separating ecological assemblages using stable isotope signals: Late Paleocene to early Eocene planktic foraminifera, DSDP Site 577, *J. Foraminiferal Res.*, *26*, 103–112.

Luciani, V., L. Giusberti, C. Agnini, J. Backman, E. Fornaciari, and D. Rio (2007), The Paleocene-Eocene thermal maximum as recorded by Tethyan planktonic foraminifera in the Forada section (northern Italy), *Mar. Micropaleontol.*, *64*, 189–214, doi:10.1016/j.marmicro.2007.05.001.

Mantovani, F., M. Panizza, E. Semenza, and S. Piacente (1978), L'Alpago (Prealpi bellunesi): Geologia, geomorfologia, nivopluvimetria, *Boll. Soc. Geol. Ital.*, *95*, 1589–1656.

Martini, E. (1971), Standard Tertiary and Quaternary calcareous nannoplankton zonation, in *Proceedings of the 2nd Planktonic Conference*, edited by A. Farinacci, vol. 2, pp. 739–785, Tecnoscienza, Rome.

Molina, E., C. Gonzalvo, M. A. Mancheño, S. Ortiz, B. Schmitz, E. Thomas, and K. von Salis (2006), Integrated stratigraphy and chronostratigraphy across the Ypresian-Lutetian transition in the Fortuna Section (Betic Cordillera, Spain), *Newsl. Stratigr.*, *42*(1), 1–19, doi:10.1127/0078-0421/2006/0042-0001.

Monechi, S., E. Angori, and K. von Salis (2000), Calcareous nannofossil turnover around the Paleocene/Eocene transition at Alamedilla (southern Spain), *Bull. Soc. Geol. Fr.*, *171*(4), 477–489, doi:10.2113/171.4.477.

Nicolo, M. J., G. R. Dickens, C. J. Hollis, and J. C. Zachos (2007), Multiple early Eocene hyperthermals: Their sedimentary expression on the New Zealand continental margin and in the deep sea, *Geology*, *35*(8), 699–702, doi:10.1130/G23648A.1.

Nomura, R., and H. Takata (2005), Data report: Paleocene/Eocene benthic foraminifers, ODP Leg 199 Sites 1215, 1220, and 1221, equatorial central Pacific Ocean [online], *Proc. Ocean Drill. Program Sci. Results, 199*, 34 pp. (Available at http://www-odp.tamu.edu/publications/199_SR/223/223.htm)

Ortiz, S., and E. Thomas (2006), Lower-middle Eocene benthic foraminifera from the Fortuna Section (Betic Cordillera, southeastern Spain), *Micropaleontology*, *52*, 97–150, doi:10.2113/gsmicropal.52.2.97.

Pagani, M., N. Pedentchouk, M. Huber, A. Sluijs, S. Schouten, H. Brinkhuis, J. S. Sinninghe Damste, G. R. Dickens, and the IODP Expedition 302 Scientists (2006), Arctic hydrology during global warming at the Palaeocene/Eocene thermal maximum, *Nature*, *442*, 671–675, doi:10.1038/nature05043.

Pearson, P. N., R. K. Olsson, B. T. Huber, C. Hemleben, and W. A. Berggren (2006), *Atlas of Eocene Planktonic Foraminiferas*, *Spec. Publ. Cushman Found. Foraminiferal Res.*, 41, 514 pp.

Perch-Nielsen, K. (1985), Cenozoic calcareous nannofossils, in *Plankton Stratigraphy*, edited by H. M. Bolli et al., pp. 427–554, Cambridge Univ. Press, New York.

Pross, J., and H. Brinkhuis (2005), Organic-walled dinoflagellate cysts as paleoenvironmental indicators in the Paleogene: A synopsis of concepts, *Palaeontol. Z.*, *79*, 53–59.

Quillévéré, F., and R. D. Norris (2003), Ecological development of acarininids (planktonic foraminifera) and hydrographic evolution of Paleocene surface waters, in *Causes and Consequences of Globally Warm Climates in the Early Paleogene*, edited by S. L. Wing et al., *Spec. Pap. Geol. Soc. Am.*, vol. 369, pp. 223–238.

Quillévéré, F., R. D. Norris, I. Moussa, and W. A. Berggren (2001), Role of photosymbiosis and biogeography in the diversification of early Paleogene acarininids (planktonic foraminifera), *Paleobiology*, *27*, 311–326, doi:10.1666/0094-8373(2001)027<0311:ROPABI>2.0.CO;2.

Quillévéré, F., R. D. Norris, D. Kroon, and P. A. Wilson (2008), Transient ocean warming and shift in carbon reservoir during the early Danian, *Earth Planet. Sci. Lett.*, *265*, 600–615, doi:10.1016/j.epsl.2007.10.040.

Raven, J., K. Caldeira, H. Elderfield, O. Hoegh-Guldberg, P. Liss, U. Riebesell, J. Shepherd, C. Turley, and A. Watson (2005), Ocean acid-

ification due to increasing atmospheric carbon dioxide, *Policy Doc. 12/05*, 60 pp., R. Soc., London.

Ravizza, G., R. N. Norris, J. Blusztajn, and M.-P. Aubry (2001), An osmium isotope excursion associated with the late Paleocene thermal maximum: Evidence of intensified chemical weathering, *Paleoceanography*, *16*, 155–163, doi:10.1029/2000PA000541.

Röhl, U., J. C. Zachos, E. Thomas, D. C. Kelly, B. Donner, and T. Westerhold (2004), Multiple early Eocene thermal maximums, *Eos Trans. AGU*, *85*(47), Fall Meet. Suppl., Abstract PP14A-02.

Röhl, U., T. Westerhold, S. Monechi, E. Thomas, J. C. Zachos, and B. Donner (2005), The third and final early Eocene thermal maximum: Characteristics, timing, and mechanisms of the ''X'' event, *Geol. Soc. Am. Abstr. Programs*, *37*(7), 264.

Schmitz, B., and V. Pujalte (2007), Abrupt increase in seasonal extreme precipitation at the Paleocene-Eocene boundary, *Geology*, *35*(3), 215–218, doi:10.1130/G23261A.1.

Schmitz, B., F. Asaro, E. Molina, S. Monechi, K. von Salis, and R. P. Speijer (1997), High-resolution iridium, $\delta^{13}C$, $\delta^{18}0$, foraminifera and nannofossil profiles across the latest Paleocene benthic extinction event at Zumaya, Spain, *Palaeogeogr. Palaeoclimatol. Palaeoecol.*, *133*, 49–68, doi:10.1016/S0031-0182(97)00024-2.

Schmitz, B., V. Pujalte, and K. Núñez-Betelu (2001), Climate and sea-level perturbations during the incipient Eocene thermal maximum: Evidence from siliciclastic units in the Basque Basin (Ermua, Zumaia and Trabakua Pass), northern Spain, *Palaeogeogr. Palaeoclimatol. Palaeoecol.*, *165*, 299–320, doi:10.1016/S0031-0182(00)00167-X.

Schouten, S., M. Woltering, W. I. C. Rijpstra, A. Sluijs, H. Brinkhuis, and J. S. Sinninghe Damsté (2007), The Paleocene-Eocene carbon isotope excursion in higher plant organic matter: Differential fractionation of angiosperms and conifers in the Arctic, *Earth Planet. Sci. Lett.*, *258*, 581–592, doi:10.1016/j.epsl.2007.04.024.

Shackleton, N. J., R. M. Corfield, and M. A. Hall (1985), Stable isotope data and the ontogeny of Paleocene planktonic foraminifera, *J. Foraminiferal Res.*, *15*, 321–337.

Sluijs, A., H. Brinkhuis, C. E. Stickley, J. Warnaar, G. L. Williams, and M. Fuller (2003), Dinoflagellate cysts from the Eocene-Oligocene transition in the Southern Ocean: Results from ODP Leg 189 [online], *Proc. Ocean Drill. Program Sci. Results, 189*, 42 pp. (Available at http://www-odp.tamu.edu/publications/189_SR/VOLUME/CHAPTERS/104.PDF)

Sluijs, A., J. Pross, and H. Brinkhuis (2005), From greenhouse to icehouse: Organic-walled dinoflagellate cysts as paleoenvironmental indicators in the Paleogene, *Earth Sci. Rev.*, *68*, 281–315, doi:10.1016/j.earscirev.2004.06.001.

Sluijs, A., G. J. Bowen, H. Brinkhuis, L. J. Lourens, and E. Thomas (2007a), The Palaeocene-Eocene thermal maximum super greenhouse: Biotic and geochemical signatures, age models and mechanisms of global change, in *Deep Time Perspectives on Climate Change: Marrying the Signal From Computer Models and Biological Proxies*, *Micropaleontol. Soc. Spec. Publ.*, vol. 2, edited by M. Williams et al., pp. 323–349, Geol. Soc., London.

Sluijs, A., H. Brinkhuis, S. Schouten, J. C. Zachos, C. M. John, S. Bohaty, J. S. Sinninghe Damsté, and E. M. Crouch (2007b), Environmental precursors to light carbon input at the Paleocene/Eocene boundary, *Nature*, *450*, 1218–1221, doi:10.1038/nature06400.

Sluijs, A., U. Röhl, S. Schouten, H.-J. Brumsack, F. Sangiorgi, J. S. Sinninghe Damsté, and H. Brinkhuis (2008a), Arctic late Paleocene–early Eocene paleoenvironments with special emphasis on the Paleocene-Eocene thermal maximum (Lomonosov Ridge, Integrated Ocean Drilling Program Expedition 302), *Paleoceanography*, *23*, PA1S11, doi:10.1029/2007PA001495.

Sluijs, A., et al. (2008b), Eustatic variations during the Paleocene-Eocene greenhouse world, *Paleoceanography*, *23*, PA4216, doi:10.1029/2008PA001615.

Speijer, R. P., and B. Schmitz (1998), A benthic foraminiferal record of Paleocene sea level and trophic/redox conditions at Gebel Aweina, Egypt, *Palaeogeogr. Palaeoclimatol. Palaeoecol.*, *137*, 79–101, doi:10.1016/S0031-0182(97)00107-7.

Stap, L., A. Sluijs, E. Thomas, and L. J. Lourens (2009), Patterns and magnitude of deep sea carbonate dissolution during Eocene thermal maximum 2 and H2, Walvis Ridge, southeastern Atlantic Ocean, *Paleoceanography*, *24*, PA1211, doi:10.1029/2008PA001655.

Sztrákos, K. (2005), Les foraminifères du Paléocène et de l'Éocène basal du sillon nord-pyrénéen (Aquitaine, France), *Rev. Micropaleontol.*, *48*, 175–236, doi:10.1016/j.revmic.2005.06.001.

Thierstein, H. R., K. R. Geitzenauer, B. Molfino, and N. J. Shackleton (1977), Global synchroneity of late Quaternary coccolith datum levels validation by oxygen isotopes, *Geology*, *5*(7), 400–404, doi:10.1130/0091-7613(1977)5<400:GSOLQC>2.0.CO;2.

Thomas, E. (1998), The biogeography of the late Paleocene benthic foraminiferal extinction, in *Late Paleocene–Early Eocene Biotic and Climatic Events in the Marine and Terrestrial Records*, edited by M.-P. Aubry, S. G. Lucas, and W. A. Berggren, pp. 214–243, Columbia Univ. Press, New York.

Thomas, E. (2005), Benthic foraminifera and early Eocene hyperthermal events (SE Atlantic Ocean), *Geol. Soc. Am. Abstr. Programs*, *37*(7), 413.

Thomas, E. (2007), Cenozoic mass extinctions in the deep sea: What disturbs the largest habitat on Earth?, in *Large Ecosystem Perturbations: Causes and Consequences*, edited by S. Monechi, R. Coccioni, and M. R. Rampino, *Spec. Pap. Geol. Soc. Am.*, vol. 424, pp. 1–23.

Thomas, E., and N. J. Shackleton (1996), The Palaeocene-Eocene benthic foraminiferal extinction and stable isotope anomalies, in *Correlation of the Early Paleogene in Northwest Europe*, edited by R. W. O. B. Knox, R. M. Corfield, and R. E. Dunay, *Geol. Soc. Spec. Publ.*, vol. 101, pp. 401–441.

Thomas, E., and J. C. Zachos (2000), Was the late Paleocene thermal maximum a unique event?, *GFF*, *122*, 169–170.

Thomas, E., J. C. Zachos, and T. J. Bralower (2000), Deep sea environments on a warm Earth: Latest Paleocene–early Eocene, in *Warm Climates in Earth History*, edited by B. T. Huber, K. G. MacLeod, and S. L. Wing, pp. 132–160, Cambridge Univ. Press, Cambridge, U. K.

Thomas, E., U. Röhl, S. Monechi, T. Westerhold, B. Balestra, and G. Morelli (2006), An early Eocene hyperthermal event at ~52.5 Ma, in *Climate and Biota of the Early Paleogene 2006, abstract volume*, edited by F. Caballero et al., p. 136, Croman, Bilbao, Spain.

Van Morkhoven, F. P. C. M., W. A. Berggren, and A. S. Edwards (1986), *Cenozoic Cosmopolitan Deep-Water Benthic Foraminifera*, *Bull. Cent. Rech. Explor. Prod. Elf Aquitaine*, vol. 11, 421 pp.

Wei, W., and S. W. Wise Jr. (1990), Biogeographic gradients of middle Eocene-Oligocene calcareous nannoplankton in the South Atlantic Ocean, *Palaeogeogr. Palaeoclimatol. Palaeoecol.*, *79*, 29–61, doi:10.1016/0031-0182(90)90104-F.

Westerhold, T., U. Röhl, J. Laskar, I. Raffi, J. Bowles, L. J. Lourens, and J. C. Zachos (2007), On the duration of magnetochrons C24r and C25n and the timing of early Eocene global warming events: Implications from the Ocean Drilling Program Leg 208 Walvis Ridge depth transect, *Paleoceanography*, *22*, PA2201, doi:10.1029/2006PA001322.

Zachos, J. C., M. Pagani, L. C. Sloan, K. Billups, and E. Thomas (2001), Trends, rhythms, and aberrations in global climate 65 Ma to present, *Science*, *292*, 686–693, doi:10.1126/science.1059412.

Zachos, J. C., et al. (2004), *Proceedings of the Ocean Drilling Program Initial Reports*, vol. 208, *Early Cenozoic Extreme Climates: The Walvis Ridge Transect*, doi:10.2973/odp.proc.ir.208.2004, Ocean Drill. Program, College Station, Tex.

Zachos, J. C., et al. (2005), Rapid acidification of the ocean during the Paleocene-Eocene thermal maximum, *Science*, *308*, 1611–1615, doi:10.1126/science.1109004.

Zachos, J. C., S. Schouten, S. Bohaty, T. Quattlebaum, A. Sluijs, H. Brinkhuis, S. J. Gibbs, and T. J. Bralower (2006), Extreme warming of mid-latitude coastal ocean during the Paleocene-Eocene thermal maximum: Inferences from TEX86 and isotope data, *Geology*, *34*(9), 737–740, doi:10.1130/G22522.1.

Zijderveld, J. D. A. (1967), AC demagnetization of rocks: Analysis of results, in *Methods in Palaeomagnetism*, edited by S. K. Runcorn, K. M. Creer, and D. W. Collinson, pp. 254–286, Elsevier, New York.

C. Agnini, E. Fornaciari, L. Giusberti, and D. Rio, Dipartimento di Geoscienze, Università di Padova, Via Giotto, 1, I-35137 Padova, Italy. (claudia.agnini@unipd.it)

J. Backman, Department of Geology and Geochemistry, Stockholm University, SE-10691 Stockholm, Sweden.

H. Brinkhuis and A. Sluijs, Palaeoecology, Laboratory of Palaeobotany and Palynology, Institute of Environmental Biology, Utrecht University, Budapestlaan 4, NL-3584 CD Utrecht, Netherlands.

V. Luciani, Dipartimento di Scienze della Terra, Polo Scientifico Tecnologico, Università di Ferrara, Via G. Saragat, 1, I-44100, Ferrara, Italy.

P. Macrì and F. Speranza, Istituto Nazionale di Geofisica e Vulcanologia, Via di Vigna Murata 605, I-00143, Roma, Italy.